applied sciences

MDPI

Article

Field Data Analysis of Pavement Marking Retroreflectivity and Its Relationship with Paint and Glass Bead Characteristics

Laura N. Mazzoni [1,*], Kamilla Vasconcelos [1], Orlando Albarracín [2], Liedi Bernucci [1] and Guilherme Linhares [3]

1 Department of Transportation Engineering, Polytechnic School of the University of São Paulo, São Paulo 05508-070, Brazil; kamilla.vasconcelos@usp.br (K.V.); liedi@usp.br (L.B.)
2 Department of Production Engineering, Mackenzie Presbyterian University, São Paulo 01221-040, Brazil; orlando.albarracin@mackenzie.br
3 Arteris S.A., São Paulo 04506-000, Brazil; guilherme.linhares@arteris.com.br
* Correspondence: laura.mazzoni@usp.br

Featured Application: White water-based paints with high-volume solids and well-graded glass beads, characterized by uniformity and curvature coefficients, improve pavement marking service life.

Abstract: Pavement marking retroreflectivity, a critical factor for safe driving, depends on the characteristics of both the paint and the embedded glass beads. However, traditional methods for predicting pavement marking service life often overlook these materials properties. This study investigates the influence of paint and glass bead characteristics on pavement marking retroreflectivity performance and addresses the characterization of glass bead size distribution by the coefficient of uniformity and curvature. Three field test sites on a Brazilian highway with various paint and glass bead combinations were evaluated. A statistical model, GAMLSS (Generalized Additive Model for Location, Scale, and Shape), was adjusted to evaluate the performance of the markings' retroreflectivity as a function of paint and glass bead characteristics. The model revealed that well-graded glass beads increased retroreflectivity by around 10%, while paints with a higher volume of solids improved service life around 65%. Therefore, the results show that acrylic water-based paints with higher volumes of solids and well-graded glass beads with better shape characteristics should be preferred to improve pavement markings' retroreflectivity and service life. The statistical model identified the key characteristics with the greatest impact on pavement marking retroreflectivity, offering valuable insights for real-world applications, which will assist pavement marking practitioners and road authorities in selecting appropriate materials to achieve enhanced durability.

Keywords: road markings; test sites; GAMLSS; particle shapes; gradation; volume solids

Citation: Mazzoni, L.N.; Vasconcelos, K.; Albarracín, O.; Bernucci, L.; Linhares, G. Field Data Analysis of Pavement Marking Retroreflectivity and Its Relationship with Paint and Glass Bead Characteristics. *Appl. Sci.* **2024**, *14*, 4205. https://doi.org/10.3390/app14104205

Academic Editors: Jue Li, Junhui Zhang, Junfeng Gao, Junhui Peng and Wensheng Wang

Received: 25 March 2024
Revised: 28 April 2024
Accepted: 29 April 2024
Published: 15 May 2024

1. Introduction

1.1. Road Safety and Pavement Markings' Retroreflectivity

During the last decades, traffic crashes have become a worldwide concern. The last UN General Assembly established the Second Decade of Action for Road Safety 2021–2030 with a target to reduce death and injuries caused by traffic by a minimum of 50% by the year 2030 [1]. The report recommends ensuring safe road use by guaranteeing that road infrastructure considers the needs of all road users and is designed to facilitate safe behaviors, including the use of clear and intuitive pavement markings [1].

Pavement markings are one of the most important features for roads due to their contribution to road safety improvement. Due to their relatively low cost and broad availability, pavement markings are a low-cost solution to reduce traffic crashes, especially in developing countries [2]. However, adequate pavement markings must present visibility during the day by the contrast of the marking material with the pavement surface, and their nighttime visibility depends on the retroreflectivity provided by the glass beads in the pavement markings.

Retroreflectivity is an engineering measure of the efficiency of the pavement markings' ability to reflect the light from vehicle's headlights back to the light source. Pavement markings' retroreflectivity is measured by the coefficient of retroreflected luminance (R_L, mcd/m^2/lx) given by the ratio of the luminance (brightness to the driver from the markings surface, mcd/m^2) and the illuminance, in lux (lx), of the vehicles' headlight on the marking [3,4]. Retroreflectivity (R_L) is most required in low-light and nighttime conditions to improve the readability and perception of the information provided by pavement markings.

The improvement and maintenance of pavement markings' retroreflectivity correlate to a reduction in traffic crash rates [3,5]. Higher values of retroreflectivity reduce the detection distance of pavement markings, especially for elderly drivers [6], which improves their reaction time. In addition, studies have shown that pavement marking retroreflectivity values higher than 200 mcd/lx/m^2 are related to a lower number of traffic crashes. Moreover, the maintenance of pavement markings' quality presents a positive effect on road safety [7].

1.2. Performance of Pavement Markings' Retroreflectivity

Pavement markings present retroreflectivity due to the glass beads applied on their surface. The characteristics of the glass beads have a great influence on the retroreflectivity levels. Smadi et al. [8] assessed the size distribution (gradation), color, shape, and air inclusion of glass beads and evaluated the influence of these properties on the initial retroreflectivity of laboratory and field samples. The authors evaluated 30 glass bead samples and could not define a definitive relationship. However, the general trends observed showed that samples with higher percentages of round and larger particles, clearer beads, and low air inclusion tended to increase the initial retroreflectivity value.

Pavement markings' retroreflectivity decreases over time. Frequent snow removal activities, traffic, and dirt accumulation scratch the glass beads' surface, which accelerates the degradation rate of retroreflectivity due to the loss of a polished surface [9]. Moreover, retroreflectivity degradation also occurs due to the loss of glass beads and dirt accumulation on the pavement markings' surface, which reduces the reflectorized area [10]. The glass beads' loss depends on the marking material used; the selection of the type of binder must consider costs and performance [11]. In addition, materials' characteristics are evaluated by laboratory tests to guarantee their quality prior to application.

Retroreflectivity values and their rates of decrease depend on the traffic volume and composition, as well as climatic conditions such as rain, solar radiation, and temperature. Due to the difficulty of reproducing traffic and weather characteristics in the laboratory, pavement markings' performance are usually evaluated by field tests [12–20]. Experimental test sites are expensive and require long periods to produce results, but they are necessary for the proper evaluation of materials' performance.

1.3. Degradation Models

The data collected from the experimental test sites provide information regarding the decrease in retroreflectivity over time, and the results can be used to predict the retroreflectivity value expected at a given time by statistical modeling. Statistical models provide details regarding the service life of pavement markings based on the variables and characteristics included to fit the data.

Prediction of the end of pavement markings' service life started during the 1990s. The initial approaches considered linear or logarithmic models to predict the retroreflectivity as a function of age and initial R_L [12,13]. The authors evaluated the retroreflectivity data from pavement markings with different marking materials, considering paints, tapes, thermoplastic, and others. Since then, statistical models and analyzed data have evolved to more complex models using machine learning methods [20]. Table 1 presents several studies from the literature that proposed statistical models with the data from experimental test sites, including the main exploratory variables and the materials considered.

Table 1. Summary of retroreflectivity prediction models in the literature.

Author/Year	Exploratory Variables Included in the Model	Materials
Zhang and Wu, 2010 [15]	Age	Tape, water-based paint, thermoplastic, and experimental materials
Hummer et al., 2011 [16]	Age and R_L initial *	Water-based paint
Robertson et al., 2013 [17]	Age, R_L initial *, lane and shoulder width, difference and R_L percentage difference, and traffic volume and cumulative traffic volume	Water-based and high-build paint
Sitzabee et al., 2013 [18]	Age, R_L initial *, traffic volume, glass bead type, and line position	Polyurea
Babić et al., 2019 [19]	Age, R_L initial *, line position, and winter maintenance	Solvent-based paint, thermoplastic, and cold plastic

* R_L initial = initial retroreflectivity value.

Most of the studies presented in Table 1 predicted retroreflectivity as a function of age and the initial retroreflectivity value. Traffic volume was also frequently included in the models as a significative variable to the degradation rate of retroreflectivity. Furthermore, with the exception of Sitzabee et al. [18], all the researchers evaluated at least two different marking materials. However, Sitzabee et al. [18] evaluated the impact of glass bead variation by comparing the performance of standard and highly reflective beads and comparing their impact on the service life of pavement markings.

Despite all the studies including more than one material type as a source of variation, none of them included an explanatory variable to describe the influence of distinct materials on the degradation rate or on the retroreflectivity value predicted. The authors adjusted different degradation models to evaluate the retroreflectivity and the degradation rate of pavement markings using different materials.In addition, the authors grouped the data based on the material type and did not present any differentiation regarding variations in the same material type, for example, by manufacturer.

1.4. Objective

It is important to quantify the impact of different paints and glass beads. The choice of different materials will change their properties and characteristics. However, existing studies in the literature fail to discuss the influence of material properties or characteristics on retroreflectivity value or pavement markings' service life. Identifying and quantifying material properties' impact on retroreflectivity degradation is crucial during material selection prior to application.

The objective of this paper is to identify the contribution of basic characteristics of paints and glass beads, evaluated through laboratory tests, on the retroreflectivity performance of pavement markings. This analysis is based on data collected at three experimental test sites at a Brazilian highway and fitted to a statistical model. The results will assist pavement marking practitioners and road authorities in selecting appropriate materials to achieve enhanced durability.

2. Materials and Methods

2.1. Materials

In this research, seven white acrylic resin water-based paints were evaluated: A, B, C, D, E, F, and G. All the paints were commercial paints, from distinct manufacturers. Paints A, B, C, D, E, and G are traditional traffic paints, whereas paint F is expected to exhibit superior performance, as indicated by the manufacturer.

The glass beads used in this study were from five distinct manufacturers: α, β, ω, δ, and ε. Two glass bead gradations (IIA and IIC), following the guidelines of Brazilian standard ABNT NBR 16184 [21], were selected from manufacturers α, β, ω, and ε. The glass beads selected from manufacturer δ were two gradations (Type 2 and Type 3) according to AASHTO M247 [22]. Figure 1 presents the grain size distribution ranges of the gradations used.

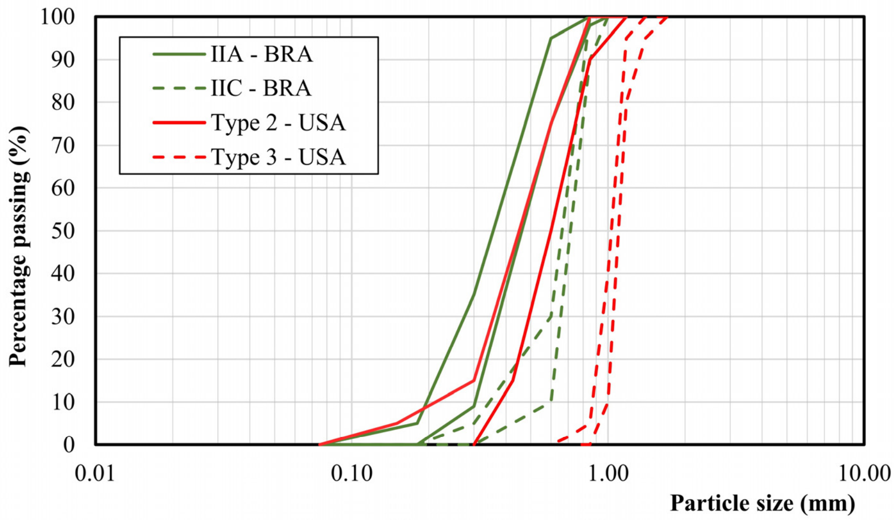

Figure 1. Grain size distribution ranges of glass beads IIA and IIC from NBR 16184 (BRA) [21] and Type 2 and Type 3 from AASHTO M247 (USA) [22].

2.2. Methods

All the paints were characterized regarding their consistency [23], specific gravity [24], and volume solids [25]. These methods were selected based on the common practices of Brazilian agencies for quality acceptance of traffic paints due to the simplicity of the tests. The glass beads' size distribution and shape characteristics were evaluated according to the procedure described in AASHTO R98 [26].

2.3. Experimental Design

The retroreflectivity data used in this study were collected from three experimental test sites where the pavement markings were subjected to the real weather and traffic conditions. Test site 1, test site 2, and test site 3 were monitored from 2016–2017, 2018–2020, and 2020–2022, respectively. All the test sites were constructed at the same road section with the same characteristics and were subjected to similar climatic conditions. Figure 2 shows the toll plaza where the test sites were located.

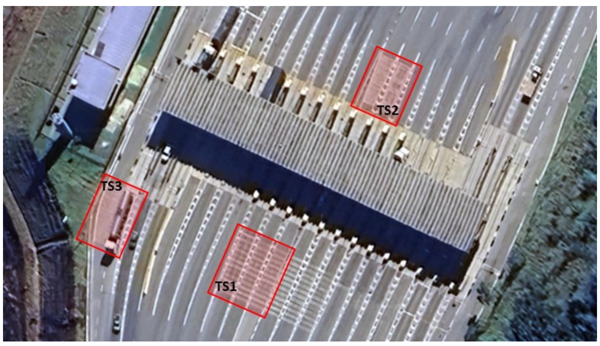

Figure 2. Experimental test site view [27].

Experiments on highways require special attention because they involve several safety aspects. The experiment used the lines transversal to traffic as recommended by NTPEP [28]. This experimental setup presents the following advantages: all stripes can be placed close together in a short length of highway, which allows for the quick measurement of retroreflectivity; all materials are subjected to the same conditions of traffic and weather; and all the stripes are hit by vehicles, which accelerates the experiment. Although transversal stripes do not represent the real condition of markings, since they are applied longitudinally [5], transversal stripes provide similar results to overall pavement markings' degradation [29,30]. Figure 3a shows one example of the test site on the day of application and Figure 3b shows the stripes after being subjected to traffic for 11 months.

(a)

(b)

Figure 3. Experimental test site 2: (**a**) day of construction; (**b**) 11 months after construction (zoomed in on the right lane).

Due to the high traffic volume of the highway, traffic interruptions for frequent retroreflectivity measurements would cause speed reductions and safety issues. Therefore, the test sites were constructed in a toll plaza rather than a free rolling section because drivers are aware and warned of a speed reduction, which avoids misunderstandings and safety issues. All the test sites were placed after the toll cabin and were subjected to the effect of vehicles' acceleration. The test sites were located on highway BR-381 (an important road in the southeastern region of Brazil with very heavy traffic of 2.27×10^7 ESALs for a 10-year project). The traffic volume at this road section is approximately 17,000 vehicles/day, of which 35% are heavy vehicles.

The retroreflectivity values were collected several times during the monitoring period and the intervals between the measurements were random due to limitations on traffic interruption or wet surfaces caused by rain. In case of rain, the data collection was rescheduled to at least 24 h after the rain ended. The measurements were collected only during the day on a dry surface with a portable retroreflectometer with 30 m geometry, as prescribed by ASTM E1710 [4]. The equipment measurement error was ±5.0%, according to the manufacturer. The retroreflectivity was measured at the positions of the right and left wheel paths and the value considered herein is the average value between both readings for each stripe. These positions were selected due to their accelerated degradation since the retroreflectivity at the wheel path tends to present values around 50% lower than the center and edges [31].

Each experimental test site used different paints, glass beads, and glass bead application rates (ARs), which generated several material combinations, as shown in Figure 4. All the paints were applied with a wet thickness of 500 µm, and no anti-skid was used.

Test site 1 was constructed in July 2016 and the retroreflectivity data were collected for 11 months until June 2017. During this period, the retroreflectivity was measured 30 times, which generated over 6500 data points. The materials evaluated were two commercial paints, A and B, and two application rates of glass beads from three different manufacturers (α, β, and ω). This study used the gradations IIA and IIC from ABNT NBR 16184 [21] (Figure 1). The selected glass bead application rates (GB-ARs) were 70% IIA + 30% IIC (7030Br) and 100% IIA (100Br), regarding the total mass of glass beads applied at a rate of 400 g/m^2. For the application at the test site, the two paints were combined with the beads available, which resulted in 12 different material combinations, as shown in Figure 4.

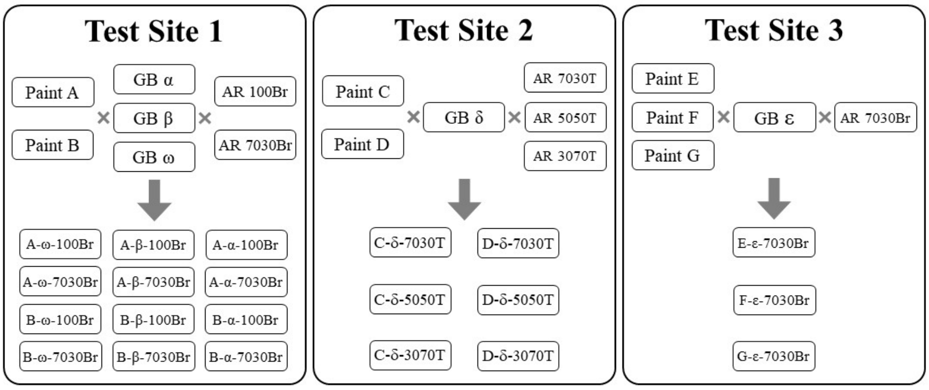

Figure 4. Experimental matrix for test sites 1, 2, and 3.

Test site 2 was constructed in September 2018 and the retroreflectivity data were monitored over 24 months until October 2020. The retroreflectivity was measured 39 times, generating over 7000 data points. The materials evaluated were two commercial paints, C and D, and three different application rates of two glass bead gradations from the same manufacturer (δ). The paints were provided by a resin manufacturer. The glass beads conformed to the AASHTO M247 [22] requirements. This study used the Type 2 and Type 3 gradations (Figure 1). The selected glass bead application rates (GB-ARs) were: 70% Type 2 + 30% Type 3 (7030T), 50% Type 2 + 50% Type 3 (5050T), and 30% Type 2 + 70% Type 3 (3070T), regarding the total mass of glass beads applied at a rate of 600 g/m^2. For the application at the test site, the two paints were combined with the three application rates, resulting in 6 different combinations, as shown in Figure 4.

Test site 3 was constructed in December 2020 and the retroreflectivity data were monitored over 18 months until August 2022. The retroreflectivity was measured 15 times, generating over 5500 data points. The materials evaluated were three commercial paints, E, F, and G, and one application rate of glass beads from one manufacturer (ε) applied at the same application rate. The glass beads followed the recommendation of Brazilian standards ABNT NBR 16184 [21] and this study used the gradations IIA and IIC in Figure 1. The selected glass bead application rate (GB-AR) was 70% IIA + 30% IIC (7030Br), regarding the total mass of glass beads applied at a rate of 400 g/m^2. For the application at the test site, the three paints were combined with the glass beads available, which resulted in 3 different material combinations, as shown in Figure 4.

3. Material Characterization Results

3.1. Paint Characterization

The paints were characterized regarding their consistency [23], specific gravity [24], and volume solids [25] prior to the application, and Table 2 presents the results.

Table 2. Basic characterization of paints.

Parameter	Limits *	Paint						
		Test Site 1		Test Site 2		Test Site 3		
		A	B	C	D	E	F	G
Consistency (KU)	$80 \leq KU \leq 95$	97	89	96	101	92	89	90
Specific gravity (g/cm^3)	$\geq$1.59	1.74	1.70	1.75	1.71	1.70	1.70	1.70
Volume solids (%)	$\geq$62.0	63.8	64.2	62.0	60.5	66.0	65.0	65.0

* Limits according to ABNT NBR 13699 [32].

The consistency results in Table 2 show that paints B, E, F, and G were in accordance with the limits required, while paints A, C, and D were out of the range. Although they are considered inadequate for use based on the specification ABNT NBR 13699 [32], the materials were used for research purposes and applied at the test sites to identify the impact of such characteristics on the paint performance. Regarding the specific gravity, all the paints were in accordance with the required value, which indicates that the paints presented adequate balance and formulation. Considering the volume solids, the parameter evaluates the percentage of the paint's volume without the volatile fraction, therefore representing the dried paint's thickness as a percentage of the wet thickness.

3.2. Glass Bead Characterization

The glass beads' size distribution and shape characteristics were evaluated according to the procedure of AASHTO R98 [26]. Figures 5–7 present the grain size distributions, thickness-to-length distributions, and sphericity distributions, respectively, for each glass bead composition and application rate.

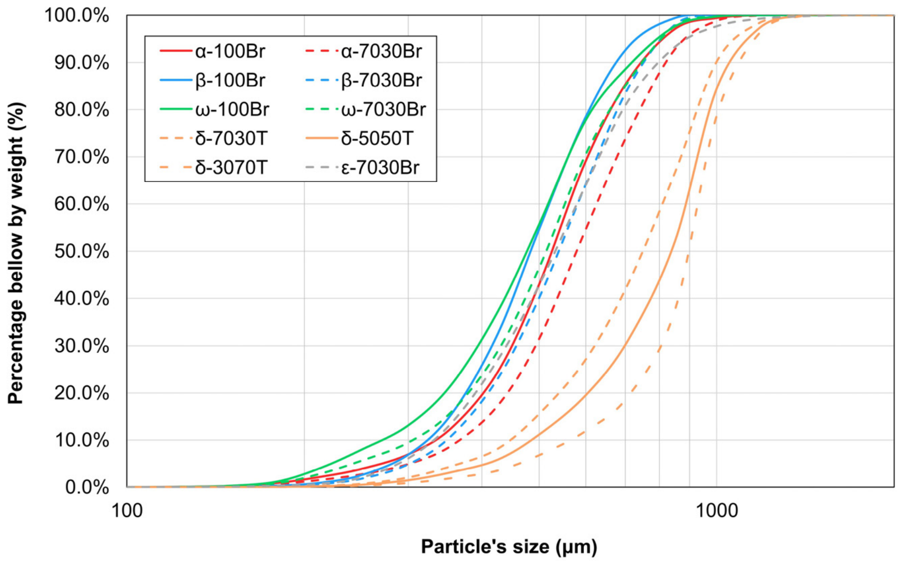

Figure 5. Grain size distributions of glass beads.

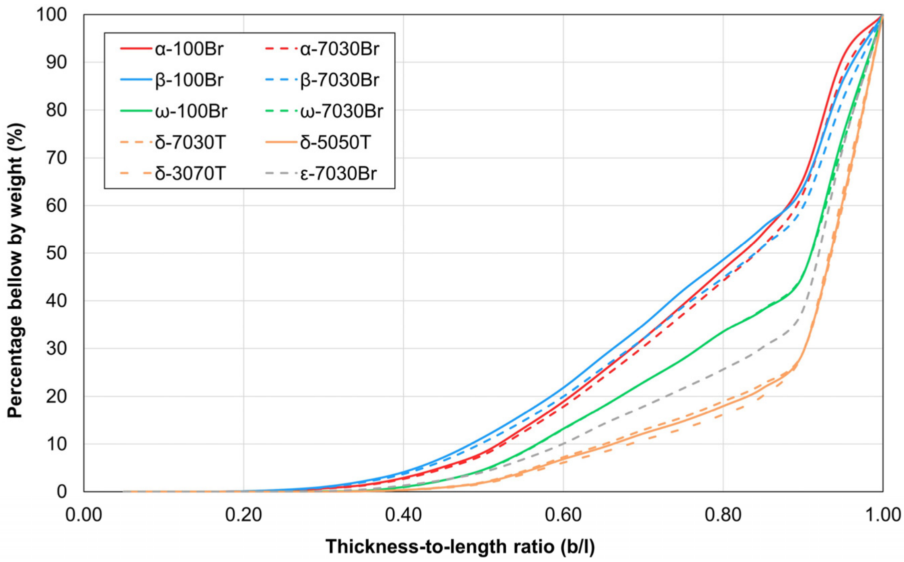

Figure 6. Thickness-to-length ratio (b/l) distributions of glass beads.

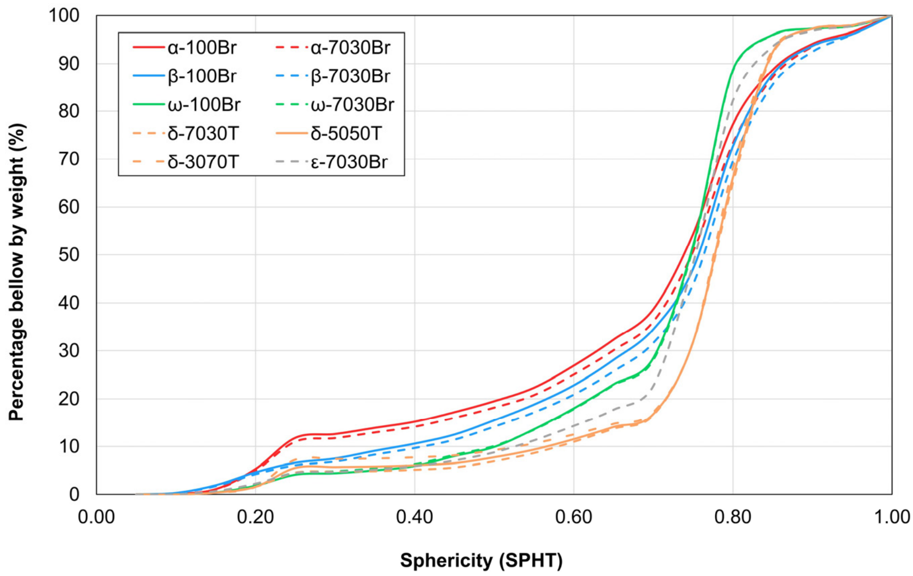

Figure 7. Sphericity (SPHT) distributions of glass beads.

The size distributions of the glass beads (Figure 5) present a large variation due to their gradations or manufacturers. The glass bead compositions δ-7030T, δ-5050T, and δ-3070T present larger particles than the other compositions. Regarding the other compositions, β-100Br and ω-100Br present the smallest particles, but all the compositions present similar size distributions.

The distributions of the thickness-to-length ratio (b/l) in Figure 6 show that compositions δ-7030T, δ-5050T, and δ-3070T present the same distribution of thickness-to-length ratio, with around 78% of round particles (b/l higher than 0.85), as required by AASHTO R98 [26]. The compositions ε-7030Br and ω-100Br present 70% and 65% of particles with b/l higher than 0.85, while the other compositions present less than 50% of round particles.

Regarding the sphericity distribution in Figure 7, all glass beads present poor shape properties considering the threshold of sphericity required by AASHTO R98 [26] to classify the particles as round (SPHT > 0.93), since all the compositions present less than 10% of round particles. Therefore, the lack of sphericity that all these glass beads present may lead to low retroreflectivity values when they are applied on the pavement markings [8,33].

Since the results of the glass bead characterization are distribution curves, the analysis of results is mainly qualitative. However, to compare the glass beads' composition and use their characteristics as variables in the statistical model, some parameters were obtained from the distributions of the grain size, thickness-to-length ratio, and sphericity to discretize the results.

The size distribution of glass beads was evaluated considering whether the composition is well graded, or not, by the coefficients of uniformity (C_U) and curvature (C_C) commonly employed in soil mechanics for analyzing granular materials [34,35]. The coefficient of uniformity is defined by Equation (1):

$$C_U = \frac{D_{10}}{D_{60}}, \quad (1)$$

where D_{10} and D_{60} correspond to the diameter (particle size) at which 10% and 60% of particles are smaller, respectively. The coefficient of uniformity (C_U) evaluates the uniformity of a granular material. The material is considered uniform if C_U is lower than 2, i.e., the particles' size distribution is concentrated at one size range. The coefficient of curvature (C_C) is described by Equation (2):

$$C_C = \frac{{D_{10}}^2}{D_{10} \times D_{60}}, \quad (2)$$

where D_{30} corresponds to the diameter (particle size) at which 30% of particles are smaller. The coefficient of curvature (C_C) identifies whether the particles' size distribution of the granular materials is continuous or not, i.e., presents a proportional percentage of several particle sizes. The material presents a continuous distribution if C_C is between 1 and 3. Continuous distribution characterizes well-graded sands and aggregates because it presents particles with several diameters that cause interlock and package between grains since the smaller particles will fill the voids between the larger particles [36]. This behavior is interesting for glass beads because a well-graded glass bead composition will present several embedment depths, which will improve the pavement markings' service life [33].

To characterize the thickness-to-length ratio curve, the parameters considered were bl_{20}, bl_{50}, and bl_{80}, which correspond to the thickness-to-length ratio at which 20%, 50%, and 80% of the particles, respectively, are lower than that value. Analogously, the characterization of the sphericity distribution curve considers the parameters $SPHT_{20}$, $SPHT_{50}$, and $SPHT_{80}$. Table 3 presents the results of the parameters used to characterize the glass beads' compositions.

Table 3. Characterization parameters for the glass beads' compositions.

Glass Bead	Parameters										
	D_{10} *	D_{30} *	D_{60} *	C_U	C_C	bl_{20}	bl_{50}	bl_{80}	$SPHT_{20}$	$SPHT_{50}$	$SPHT_{80}$
α-7030Br	0.368	0.489	0.625	1.698	1.040	0.62	0.84	0.93	0.53	0.75	0.82
α-100Br	0.335	0.450	0.557	1.663	1.085	0.61	0.82	0.92	0.51	0.74	0.81
β-7030Br	0.348	0.457	0.577	1.658	1.040	0.60	0.84	0.94	0.59	0.76	0.83
β-100Br	0.323	0.415	0.520	1.610	1.025	0.57	0.81	0.93	0.56	0.75	0.82
ω-7030Br	0.305	0.430	0.553	1.813	1.096	0.67	0.91	0.98	0.62	0.74	0.78
ω-100Br	0.270	0.494	0.518	1.919	1.745	0.67	0.91	0.98	0.62	0.74	0.78
δ-7030T	0.447	0.620	0.810	1.812	1.062	0.81	0.93	0.97	0.71	0.77	0.82
δ-5050T	0.485	0.698	0.886	1.827	1.134	0.83	0.93	0.97	0.71	0.77	0.82
δ-3070T	0.568	0.805	0.928	1.634	1.229	0.85	0.93	0.97	0.71	0.77	0.82
ε-7030Br	0.348	0.457	0.577	1.658	1.040	0.60	0.84	0.94	0.59	0.76	0.83

* Diameter in mm.

The glass beads are fine granular materials with their particles' size distribution inside a small size range. Therefore, glass beads present uniform size distribution with C_U values varying from 1.6 to 2.0. The glass beads also present well-graded (continuous) gradation, confirmed by the C_C, which is desirable for proper retroreflectivity performance over time.

4. Test Site Results: Statistical Analysis

The data collected at experimental test sites 1, 2, and 3 yielded over 19,000 retroreflectivity values, encompassing the characteristics of paints, glass beads, and the test site itself. Relying solely on graphical analysis for evaluating pavement markings' performance would introduce bias into the qualitative analysis results. To ensure a robust results analysis and to quantify the impact of each variable on retroreflectivity values and pavement markings' performance, statistical analysis was conducted.

In this section, the Generalized Additive Models for Location, Scale, and Shape (GAMLSSs) are implemented due to their flexibility in addressing a wide range of distributions and incorporating random effects to account for data correlation [37,38]. The GAMLSSs can be understood as an extension of the Generalized Linear Models (GLMs). The model was adjusted and its parameters were estimated using the *gamlss* library of the software R version 4.2.2 [39].

In the descriptive analysis, it was observed that the distribution of retroreflectivity is positively skewed. Therefore, a Weibull distribution was considered in this study to be suitable for modeling the positive random variable (retroreflectivity) representing values until the end of service. It is worth noting that the normal distribution did not fit the data well, as expected based on the data distribution. Let y'_{ijk} be a vector representing the retroreflectivity observed for i paint characteristics during a j time period of days after painting at the k test site. Conditional on the random effects u, assume that the elements of y are independent and follow a Weibull distribution.

Thus, the Weibull regression model considered is described by Equation (3):

$$\begin{aligned} & Y_{ij} \middle| u \sim \text{Weibull}(.) \\ \ln\left(\mu_{ijk}\right) = (\theta_0 + u_k) + \sum_{j=1}^{8} \theta_{1,j} X_{t,j} + \theta_2 X_{v.sol} + \theta_3 X_{bl50} + \theta_4 X_{CU} + \theta_5 X_{CC} + \theta_6 X_{spht_{20}} \\ + \sum_{j=1}^{8} \theta_{7,j} X_{t,j \times v.sol} + \theta_8 X_{CU \times CC}, \end{aligned} \tag{3}$$

where μ_{ijk} is the mean of the response variable related to the explanatory variables through the logarithm link function. The explanatory variables considered in this study are paints' volume solids ($X_{v.sol}$), glass beads' coefficient of uniformity (X_{CU}), coefficient of curvature (X_{CC}), and shape characteristics ($X_{spht_{20}}$ and $X_{bl_{50}}$), and the dichotomous time variables $X_{t,1}$ = (0, 20], $X_{t,2}$ = (20, 40], $X_{t,3}$ = (40, 60], $X_{t,4}$ = (60, 80], $X_{t,5}$ = (80, 100], $X_{t,6}$ = (100, 200], $X_{t,7}$ = (200, 300], and $X_{t,8}$ = (300, 800), which represent the time periods (days elapsed since the test site construction) during which retroreflectivity was observed. Note that parentheses brackets indicate an open interval, not including a start point, while a closed interval includes the end point and is denoted with the square brackets, as a mathematical notation. Thus, if $X_{t,j} = 1$, the retroreflectivity was mensurated in the first 20 days of application of the pavement marking; the other time variables assume a value of zero in this case. Categorizing the time variable helps to evaluate changes in the degradation rate of pavement markings over time, which is not linear. It is important to highlight that the variable time accounts for the effect of traffic and weather on the pavement marking degradation.

The continuous variables $X_{v.sol}$, X_{CU}, X_{CC}, and $X_{bl_{50}}$ represent the values of these properties obtained from the characterization tests. On the other hand, the variable $X_{spht_{20}}$ is dichotomous and assumes a value of one when the $SPHT_{20}$ of the paint is higher than 0.59, or zero otherwise. Finally, the $\theta' = (\theta_0, \ldots, \theta_8)$ vector represents the fixed parameters to be estimated using maximum likelihood [37,38], and the random intercept $u_k \text{with} k = 1, 2, 3$ was considered to deal with the variability of the measurement at a distinct test site.

During the model selection process, other variables, such as paint consistency and density, were considered. However, these variables were insignificant to the model (*p*-value > 0.05). Therefore, only variables contributing to the model significance were included in Equation (3). In addition, interactions between explanatory variables were also considered. Interactions evaluate whether the association between the target variable and the independent variable varies based on the value of another independent variable. The interactions between all variables were considered in the model.

The final model presented in Equation (3) includes the variables and interactions selected using a stepwise algorithm based on the Akaike information criterion (AIC) [37,38]. The interpretability of the final model was also considered during the selection process. It is worth noting that a data cleansing process was conducted on the retroreflectivity dataset with the intention of removing any typos or outliers. Retroreflectivity values lower than 70 $mcd/m^2/lx$ were also excluded from the dataset to simulate an experiment, using as the interruption criteria the end of service life as considered by the MUTCD [40].

4.1. Model Adjustment

The data was adjusted to the model proposed in Equation (3), and the parameters were estimated using the *gamlss* library of the software R [39]. Table 4 presents the estimates of the parameters, their standard errors, and the *p*-values. All variables were found to be significant at a 5.0% significance level. Despite the variable $X_{v.sol}$ not being significant, it was kept in the model due to its significant interaction with time.

To validate the adequacy of the fitted model, a residual analysis was run, and Figure 8 presents the diagnostic plots of the normalized randomized quantile residuals [41]. The diagnostic plots in Figure 8 show that there is no violation of the model assumptions, and the residuals are normally distributed, confirming the adequacy of the fitted data to the model.

Table 4. The model's estimated parameters.

	Variable	Parameter	Estimate	Standard Error	*p*-Value
Main effects	Intercept	θ_0	−7.330	0.362	<0.001
	$X_{t,2}$: (20, 40]	$\theta_{1,2}$	−5.850	0.640	<0.001
	$X_{t,3}$: (40,60]	$\theta_{1,3}$	−8.822	0.587	<0.001
	$X_{t,4}$: (60,80]	$\theta_{1,4}$	−8.281	0.720	<0.001
	$X_{t,5}$: (80,100]	$\theta_{1,5}$	−10.195	0.612	<0.001
	$X_{t,6}$: (100,200]	$\theta_{1,6}$	−11.199	0.421	<0.001
	$X_{t,7}$: (200,300]	$\theta_{1,7}$	−11.308	0.590	<0.001
	$X_{t,8}$: (300,800]	$\theta_{1,8}$	−88.414	0.627	<0.001
	V.sol	θ_2	−0.003	0.005	0.404
	bl_{50}	θ_3	0.011	0.005	<0.001
	C_U	θ_4	6.652	0.113	<0.001
	C_C	θ_5	9.055	0.150	<0.001
	$SPHT_{20}$	θ_6	0.186	0.054	<0.001
Interactions	V.sol × $X_{t,2}$: (20, 40]	$\theta_{7,2}$	0.090	0.010	<0.001
	V.sol × $X_{t,3}$: (40,60]	$\theta_{7,3}$	0.133	0.009	<0.001
	V.sol × $X_{t,4}$: (60,80]	$\theta_{7,4}$	0.118	0.011	<0.001
	V.sol × $X_{t,5}$: (80,100]	$\theta_{7,5}$	0.148	0.010	<0.001
	V.sol × $X_{t,6}$: (100,200]	$\theta_{7,6}$	0.159	0.007	<0.001
	V.sol × $X_{t,7}$: (200,300]	$\theta_{7,7}$	0.156	0.010	<0.001
	V.sol × $X_{t,8}$: (300,800]	$\theta_{7,8}$	0.120	0.010	<0.001
	$C_U \times C_C$	θ_8	−4.841	0.078	<0.001

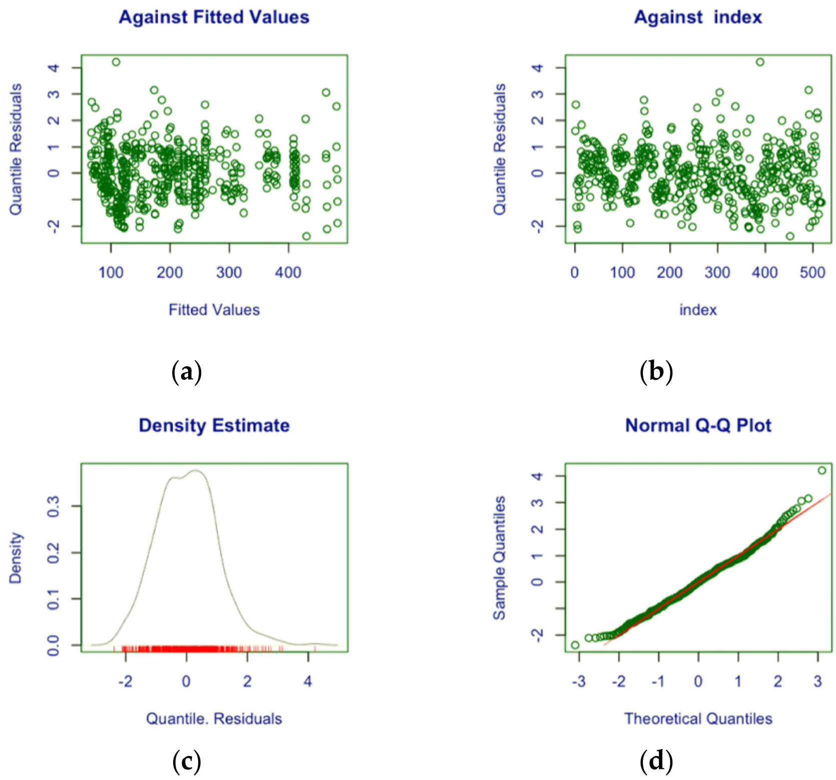

Figure 8. Model's diagnostic plots: (**a**) Residuals × Fitted Values; (**b**) Residuals × Index; (**c**) Residuals distribution; (**d**) Normal Q-Q plot.

4.2. Results Analysis

Given the model results, the coefficients obtained may be interpreted to analyze the variables' impact on the average retroreflectivity. It is worth mentioning that in the time variable, the category $X_{t,1} = (0, 20]$ is the reference category. Therefore, the effects of the other time variables are interpreted in comparison to $X_{t,1}$.

Regarding the covariates without interactions, it is noteworthy that the parameter estimates for the $X_{bl_{50}}$ and $X_{spht_{20}}$ variables are positive, indicating that an increase in their values is associated with an increase in the mean retroreflectivity. Enhancing the roundness of glass beads (X_{bl50}) by 0.1 results in an average increase of 11.59% in retroreflectivity because $\exp(\theta_3 \times X_{bl_{50}}) - 1 = \exp(0.011 \times 0.1 \times 100) - 1 = 0.1159$. Analogously, the impact of glass beads' sphericity on the pavement markings may be calculated as $\exp\left(\theta_6 \times X_{spht_{20}}\right) - 1 = \exp(0.186 \times 1) - 1 = 0.205$, i.e., pavement markings with glass beads with a sphericity higher than 0.59 present retroreflectivity, on average, 20.5% higher when compared to pavement markings with glass beads with sphericity lower than 0.59. These parameters characterize the glass beads' shape, and the results confirm the importance of shape to retroreflectivity [8].

To analyze the impact of C_U and C_C on retroreflectivity, it is necessary to consider the interaction between these variables. The size and gradation of glass beads also impact the retroreflectivity. However, an evaluation of glass beads' size and gradation beyond the granulometric curves or even the quantification of different beads' gradation on retroreflectivity was not found in the literature. Therefore, the evaluation of the coefficients related to C_U and C_C is important to understand the grain size distribution contribution to retroreflectivity. Since there is an interaction between C_U and C_C, their impact on retroreflectivity must be evaluated simultaneously.

A higher coefficient of uniformity indicates a large range of sizes for glass beads, while higher coefficient of curvature indicates the equivalent distribution of several particles' sizes. The increase in retroreflectivity related to higher C_U and C_C values shows the importance of selecting well graded glass beads. The improvement of retroreflectivity occurs due to the distribution of several glass bead sizes on the pavement markings' surface since the larger particles fall on the paint surface first, and then the smaller particles fill the voids between the larger beads, which expands the area of the markings covered with glass beads. Thus, there is a higher area available to reflect light and improve the night visibility of pavement markings [10].

Supposing a glass bead sample with X_{CU} = 1.700, an increase in X_{CC} by 0.1 will improve the retroreflectivity, on average, by 8.71%. The difference between the R_L before ($X_{CC_1} = 1.0$) and after the C_C increase ($X_{CC_2} = 1.1$) may be calculated as $\exp\left[(\theta_4 \times X_{CU} + \theta_5 \times X_{CC_2} - \theta_8 \times X_{CU} \times X_{CC_2}) - (\theta_4 \times X_{CU} + \theta_5 \times X_{CC_1} - \theta_8 \times X_{CU} \times X_{CC_1})\right] - 1 = \exp\left[(6.652 \times 1.700 + 9.055 \times 1.1 - 4.841 \times 1.700 \times 1.1) - (6.652 \times 1.700 + 9.055 \times 1.0 - 4.841 \times 1.700 \times 1.0)\right] - 1 = 8.71\%$.

Regarding the paint's characteristics, the effect of the variable $X_{v.sol}$ on the retroreflectivity is analyzed considering the different time periods in which the retroreflectivity was measured. An increase of one unit in the volume of solids leads to an average decrease in retroreflectivity of 0.23% when measured within 20 days after the application of the pavement marking. However, this decrease is not statistically significant (p-value = 0.404).

The volume solids of paints are associated with pavement markings' durability. The estimates of the parameters of the time intervals obtained at the model adjustment show that the decrease in retroreflectivity over time depends on the volume solids. Supposing a pavement marking using a paint with V.sol = 62.0, the retroreflectivity decreases, on average, by 24.38% ($\exp(\theta_4 \times X_{t,2} + \theta_{7,2} \times X_{t,2} \times X_{V.sol}) - 1 = \exp(-5.850 \times 1 + 0.090 \times 1 \times 62) - 1 = 0.2438$) at the time interval $X_{t,2}$= (20, 40] when compared to the initial time interval. Analogously, the time interval $X_{t,3}$ = (40, 60] presents, on average, 43.50% lower retroreflectivity values. Regarding the other time intervals, the reduction in retroreflectivity is, on average, 62.36% for $X_{t,4}$ = (60, 80], 63.51% for $X_{t,5}$ = (80,100], 74.08% for $X_{t,6}$ = (100,200], 80.30% for $X_{t,7}$ = (200,300], and 74.64% for $X_{t,8}$ = (300,800). The volume solids is an important characteristic because it evaluates the percentage of paint's volume without the volatile fraction, thus representing the percentage of the dried paint's thickness compared to the wet thickness. Therefore, this parameter influenced the retroreflectivity over time instead of the initial retroreflectivity.

Retroreflectivity decreases progressively over time, but the model's estimated parameters show that the reduction over time is not linear. There is a severe decrease for the first 100 days (until $X_{t,5}$) and a relative continuous reduction for the other time intervals. However, the retroreflectivity reduction is more intense for the time interval $X_{t,7}$ than the time interval $X_{t,8}$, which shows that the estimated retroreflectivity is higher for interval $X_{t,8}$ than $X_{t,7}$. This occurs because the evaluation of time as an interval accounts for the seasonal variation of retroreflectivity, which may present higher values after rain due to surface cleaning, as reported by Salles et al. [42].

Considering a one-unit increase in the volume solids of paints, the retroreflectivity improves by 9.15% when it shifts from being measured within the time interval $X_{t,1} = (0, 20]$ to being measured within the interval $X_{t,2} = (20, 40]$. Analogously, the average retroreflectivity improvement is, on average, 14.0%, 12.3%, 15.7%, 17.0%, 16.6%, and 12.6% for time intervals $X_{t,3}$, $X_{t,4}$, $X_{t,5}$, $X_{t,6}$, $X_{t,7}$, and $X_{t,8}$, respectively.

The positive contribution of volume solids to the average retroreflectivity shows that the retroreflectivity decreases slower for paints with higher volume solids, i.e., higher volume solids paints reduce the degradation rate of pavement markings' retroreflectivity.

An increase in paints' volume solids contributes to the occurrence of the retroreflectivity peak and improves the expected service life of pavement markings. The V.sol is responsible for the thickness of the paints' film on the pavement surface after the drying of paint. Higher V.sol leads to higher dry paint thickness compared to lower V.sol paints if they are applied at the same wet thickness. Therefore, the glass beads present higher embedment depths that will require more wear to remove the particles from the markings' surface, which improves the service life of pavement markings.

Finally, random effects were incorporated into the model to deal with the variability between the test sites. The random effect in the intercept for the variable u_k refers to each test site, in which $u_1 = -0.1097$ for test site 1, $u_2 = -0.0082$ for test site 2, and $u_3 = 0.1179$ for test site 3. The intercepts indicates that the retroreflectivity values were, on average, higher for test site 3, followed by test site 2 and test site 1, respectively. The results show that, even with the higher concentration of glass beads at test site 2 (600 g/m^2), the retroreflectivity values were most impacted by material characteristics.

5. Discussion

This research evaluated three experimental test sites of pavement markings in a Brazilian road and proposed a statistical model to assess the quantitative impact of the characteristics of the water-based paints with acrylic resin and the characteristics of the glass beads used on the retroreflectivity value over time for the test sites. The analysis of the coefficients' estimates was important to quantify the impact of each materials' characteristic on the retroreflectivity and on the pavement markings' service life.

5.1. Glass Bead Characteristics

The glass beads' shape has a strong impact on the initial retroreflectivity of the pavement markings [8]. Regarding the coefficients of the properties of shape, both bl_{50} and $SPHT_{20}$ present a positive impact on the retroreflectivity; however, the $SPHT_{20}$ has a stronger contribution to the retroreflectivity improvement than bl_{50}. In addition, the glass beads evaluated in this research present poor shape properties considering the threshold of sphericity to classify the particles as round (SPHT > 0.93), while a much larger percentage of particles for all glass beads may be classified as round considering the thickness-to-length ratio (b/l > 0.85). Therefore, considering the glass beads evaluated herein, they meet the requirements of shape, b/l > 0.85, more easily than the requirements for sphericity, SPHT > 0.93. Moreover, SPHT is harder to achieve and has a higher impact on the retroreflectivity. Thus, it is recommended that the glass beads evaluated herein should present better shape characteristics, mainly sphericity.

The previous study reporting the impact of glass bead gradation on pavement markings' retroreflectivity also discretized the size distribution, but evaluated it as a rank between the samples evaluated [8]. This research calculated and attributed two coefficients commonly used to classify granular materials in soil mechanics, the coefficients of uniformity (C_U) and curvature (C_C), to characterize the size distribution of each glass bead sample. The results of both coefficients are in a short range, which might indicate the need of proposing a specific classification range for glass beads. Ultimately, the estimates of the model's coefficients showed that the improvement of glass beads' gradation by C_C is more important than the uniformity (C_U). The coefficients could evaluate, discretize, and differentiate the glass beads' size distributions.

Based on the results, the expected coefficient of uniformity for glass beads must range around 1.5 to 1.9 to guarantee the absence of fine particles that reduce the retroreflectivity or larger particles that will cause a lack of embedment depth and premature failure of pavement markings. Regarding the coefficient of curvature, the results obtained range around 1.05 to 1.20; this may be an adequate range to guarantee a well-graded glass bead to improve R_L. It is important to highlight that these ranges are only premises based on the results obtained herein. However, it is recommended to calculate the C_U and C_C for other glass beads to observe how they impact the retroreflectivity and evaluate whether the coefficients can be used to create a new range or not.

5.2. Paint Characteristics

The paints were evaluated regarding their consistency, specific gravity, and volume solids. In order to fit the data to the statistical model proposed in this research, the only significant variable was the volume solids. An increase in this variable causes a non-significant reduction in the initial retroreflectivity; however, considering the interaction with time, an increase in volume solids reduces the degradation rate of retroreflectivity over time, i.e., improves the service life of pavement markings.

Despite the limitation of using only the volume solids as a paint characteristic, the model captured the expected tendency of retroreflectivity. It is important to highlight that other characteristics of paints impact pavement markings' retroreflectivity. The results obtained by the analysis of the model's coefficients show that using white water-based paints with acrylic resin and higher volume solids could improve pavement markings' performance, i.e., considering commercial paints with similar characteristics, in which it is not possible to adjust the formulation, the one with higher volume solids should be chosen because it may present a better performance over time.

6. Conclusions

This research analyzed the retroreflectivity data collected from pavement markings at Brazilian test sites under real traffic action subjected to tropical climate conditions. It adjusted a statistical model to evaluate the influence of paint and glass bead characteristics on pavement markings' service life.

The research demonstrated the importance of the proper characterization of paints and glass beads before field application. Paints' volume solids are an important characteristic for pavement markings' durability since higher values of volume solids in paints were found to enhance pavement markings' durability. Regarding the glass beads, the results emphasize the importance of their shape on the initial retroreflectivity. Moreover, the research addresses the characterization of glass beads' size distribution as a discrete value, facilitating comparison based on gradation.

The research findings offer guidance for pavement marking practitioners and road authorities in selecting materials. By understanding the impact of paint characteristics and glass bead properties on retroreflectivity, practitioners can make informed choices regarding suitable paint and glass beads. Moreover, improving pavement markings' service life reduces the maintenance frequency and, consequently, reduces road safety issues.

From the results obtained, it is possible to conclude that white water-based paints with higher volume solids are preferable for improving pavement markings' service life. In addition to the importance of glass beads' shape characteristics regarding sphericity

(SPHT) and thickness-to-length ratio (b/l), it is also recommended to characterize the glass beads' grain size distribution by the coefficients of uniformity and curvature.

It is important to emphasize that this research does not aim to reduce or replace the characterization tests of paints and glass beads. Rather, it evaluates which parameters most significantly affect the retroreflectivity to improve the acceptance limits of these materials. Furthermore, the results obtained herein are based on a restricted number of materials subjected to specific climate conditions and traffic. Therefore, the application of this research must be carefully conducted, considering only white acrylic water-based paints and glass beads with characteristics similar to those evaluated herein.

Author Contributions: Conceptualization, L.N.M. and L.B.; methodology, L.N.M., O.A., G.L. and K.V.; validation, L.N.M. and O.A.; formal analysis, L.N.M., K.V., O.A. and L.B.; resources, L.B., K.V. and G.L.; writing—original draft preparation, L.N.M. and O.A.; writing—review and editing, L.N.M., K.V., L.B., O.A. and G.L.; visualization, L.N.M., G.L. and O.A.; supervision, K.V. and L.B.; project administration, L.B.; funding acquisition, L.B., K.V. and G.L. All authors have read and agreed to the published version of the manuscript.

Funding: This study was funded in part by the Coordenação de Aperfeiçoamento de Pessoal de Nível Superior-Brasil (CAPES)-Finance Code 001 and by Recurso para Desenvolvimento Tecnológico (RDT) from concessionary Autopista Fernão Dias with the supervision of Agência Nacional de Transportes Terrestres (ANTT).

Institutional Review Board Statement: Not applicable.

Informed Consent Statement: Not applicable.

Data Availability Statement: Restrictions apply to the availability of these data. Data were obtained from Autopista Fernão Dias and are available from the authors with the permission of Autopista Fernão Dias.

Conflicts of Interest: Author Guilherme Linhares was employed by the company Arteris S.A. The remaining authors declare that the re-search was conducted in the absence of any commercial or financial relationships that could be construed as a potential conflict of interest.

References

1. WHO-World Health Organization. *Global Plan for the Decade of Action for Road Safety 2021–2030*; World Health Organization: Geneva, Switzerland, 2021.
2. Burghardt, T.E.; Mosböck, H.; Pashkevich, A.; Fiolić, M. Horizontal Road Markings for Human and Machine Vision. In *Proceedings of the Transportation Research Procedia*; Elsevier: Amsterdam, The Netherlands, 2020; Volume 48.
3. Smadi, O.; Souleyrette, R.R.; Ormand, D.J.; Hawkins, N. Pavement Marking Retroreflectivity Analysis of Safety Effectiveness. *Transp. Res. Rec.* **2008**, *2056*, 17–24. [CrossRef]
4. *E1710-11*; Standard Test Method for Measurement of Retroreflective Pavement Marking Materials with CEN-Prescribed Geometry Using a Portable. American Society for Testing and Materials: West Conshohocken, PA, USA, 2011.
5. Carlson, P.J.; Park, E.S.; Kang, D.H. Investigation of Longitudinal Pavement Marking Retroreflectivity and Safety. *Transp. Res. Rec.* **2013**, *2337*, 59–66. [CrossRef]
6. Guan, Y.; Hu, J.; Wang, R. Study on the Enrichment of Pavement Marking Width and Retroreflectivity on Elderly Drivers' Safety. *Transp. Res. Rec.* **2024**. [CrossRef]
7. Babić, D.; Fiolić, M.; Babić, D.; Gates, T. Road Markings and Their Impact on Driver Behaviour and Road Safety: A Systematic Review of Current Findings. *J. Adv. Transp.* **2020**, *2020*, 1–19. [CrossRef]
8. Smadi, O.; Hawkins, N.; Aldemir-Bektas, B.; Carlson, P.; Pike, A.; Davies, C. Recommended Laboratory Test for Predicting the Initial Retroreflectivity of Pavement Markings from Glass Bead Quality. *Transp. Res. Rec. J. Transp. Res. Board* **2014**, *2440*, 94–102. [CrossRef]
9. Wenzel, K.M.; Burghardt, T.E.; Pashkevich, A.; Buckermann, W.A. Glass Beads for Road Markings: Surface Damage and Retroreflection Decay Study. *Appl. Sci.* **2022**, *12*, 2258. [CrossRef]
10. Zhang, G.; Hummer, J.E.; Rasdorf, W. Impact of Bead Density on Paint Pavement Marking Retroreflectivity. *J. Transp. Eng.* **2010**, *136*, 773–781. [CrossRef]
11. Babić, D.; Burghardt, T.E.; Babić, D. Application and Characteristics of Waterborne Road Marking Paint. *Int. J. Traffic Transp. Eng.* **2015**, *5*, 150–169. [CrossRef]
12. Andrady, A.L. *Pavement Marking Materials: Assessing Environment Friendly Performance*; National Academy Press: Washington, DC, USA, 1997; ISBN 0309060648.

13. Lee, J.T.; Maleck, T.L.; Taylor, W.C. Pavement Marking Material Evaluation Study in Michigan. *ITE J. Institute Transp. Eng.* **1999**, *69*, 44.
14. Abboud, N.; Bowman, B.L. Cost- and Longevity-Based Scheduling of Paint and Thermoplastic Striping. *Transp. Res. Rec.* **2002**, *1974*, 55–62. [CrossRef]
15. Zhang, Y.; Wu, D. Methodologies to Predict Service Lives of Pavement Marking Materials. *J. Transp. Res. Forum* **2010**, *45*, 5–18. [CrossRef]
16. Hummer, J.E.; Rasdorf, W.; Zhang, G. Linear Mixed-Effects Models for Paint Pavement-Marking Retroreflectivity Data. *J. Transp. Eng.* **2011**, *137*, 705–716. [CrossRef]
17. Robertson, J.; Sarasua, W.; Johnson, J.; Davis, W. A Methodology for Estimating and Comparing the Lifecycles of High-Build and Conventional Waterborne Pavement Markings on Primary and Secondary Roads in South Carolina. *Public Work. Manag. Policy* **2013**, *18*, 360–378. [CrossRef]
18. Sitzabee, W.E.; White, E.D.; Dowling, A.W. Degradation Modeling of Polyurea Pavement Markings. *Public Work. Manag. Policy* **2013**, *18*, 185–199. [CrossRef]
19. Babić, D.; Ščukanec, A.; Babić, D.; Fiolić, M. Model for Predicting Road Markings Service Life. *Balt. J. Road Bridg. Eng.* **2019**, *14*, 341–359. [CrossRef]
20. Mousa, M.R.; Mousa, S.R.; Hassan, M.; Carlson, P.; Elnaml, I.A. Predicting the Retroreflectivity Degradation of Waterborne Paint Pavement Markings Using Advanced Machine Learning Techniques. *Transp. Res. Rec.* **2021**, *2675*, 483–494. [CrossRef]
21. *NBR 16184:2021*; Sinalização Horizontal Viária—Esferas e Microesferas de Vidro—Requisitos e Métodos de Ensaio. Associação Brasileira de Normas Técnicas:: Rio de Janeiro, RJ, Brazil, 2021.
22. *AASHTO M247-13*; Standard Specification for Glass Beads Used in Pavement Markings. American Association of State Highway and Transportation Officials: Washington, DC, USA, 2013.
23. *D562-14*; Standard Test Method for Consistency of Paints Measuring Krebs Unit (KU) Viscosity Using a Stormer-Type Viscometer. American Society for Testing and Materials: West Conshohocken, PA, USA, 2014.
24. *D1475-13*; Standard Test Method for Density of Liquid Coatings, Inks, and Related Products. American Society for Testing and Materials: West Conshohocken, PA, USA, 2013.
25. *D2792-17*; Standard Practice for Solvent and Fuel Resistance of Traffic Paint. American Society for Testing and Materials: West Conshohocken, PA, USA, 2017.
26. *AASHTO R98-20*; Standard Practice for Standard Practice for Determination of Size and Shape of Glass Beads Used in Traffic Markings by Means of Computerized Optical Method. American Association of State Highway and Transportation Officials: Washington, DC, USA, 2020.
27. Google Earth 10.49.0.0 Test Site View (22°54′31″ S 46°25′29″ W). Available online: https://www.google.com/earth/about/ (accessed on 12 March 2024).
28. NTPEP. *NTPEP Best Practices Manual*; American Association of State Highway and Transportation Officials: Washington, DC, USA, 2004.
29. Zhang, Y.L.; Pike, A.M.; Ge, H.C.; Carlson, P.J. Comparison of Designs of Field Test Decks for Pavement Marking Materials. *Transp. Res. Rec.* **2011**, *5*, 95–102. [CrossRef]
30. Pike, A.M.; Songchitruksa, P. Predicting Pavement Marking Service Life with Transverse Test Deck Data. *Transp. Res. Rec. J. Transp. Res. Board* **2015**, *2482*, 16–22. [CrossRef]
31. Mazzoni, L.N.; Ho, L.L.; Vasconcelos, K.L.; Bernucci, L.L.B. Probabilistic Service Life Model of Pavement Marking by Degradation Data. *Transp. Res. Rec.* **2022**, *2676*, 328–340. [CrossRef]
32. *NBR 13699:2021*; Sinalização Horizontal Viária-Tinta à Base de Resina Acrílica Emulsionada Em Água. Associação Brasileira de Normas Técnicas: Rio de Janeiro, RJ, Brazil, 2021.
33. Migletz, J.; Fish, J.K.; Graham, J.L. *Roadway Delineation Practices Handbook*; Federal Highway Administration: Washington, DC, USA, 1994.
34. Chai, X.; Sheng, Y.; Liu, J.; Xu, Y.; Liu, H. Experimental Study on the Mechanical Properties of Saturated Tailing Sand with Different Particle Sizes. *Appl. Sci.* **2022**, *12*, 12231. [CrossRef]
35. Daghistani, F.; Abuel-Naga, H. Evaluating the Influence of Sand Particle Morphology on Shear Strength: A Comparison of Experimental and Machine Learning Approaches. *Appl. Sci.* **2023**, *13*, 8160. [CrossRef]
36. Pinto, C. *De S. Curso Básico de Mecânica Dos Solos*, 3rd ed.; Oficina dos Textos: São Paulo, SP, Brazil, 2006.
37. Stasinopoulos, M.D.; Rigby, R.A.; Heller, G.Z.; Voudouris, V.; De Bastiani, F. *Flexible Regression and Smoothing: Using GAMLSS in R*; CRC Press: Chapman and Hall/CRC: New York, NY, USA, 2017; ISBN 1351980378.
38. Rigby, R.A.; Stasinopoulos, M.D.; Heller, G.Z.; De Bastiani, F. *Distributions for Modeling Location, Scale, and Shape: Using GAMLSS in R*; Chapman and Hall/CRC: New York, NY, USA, 2019; ISBN 0429298544.
39. Stasinopoulos, D.M.; Rigby, R.A. Generalized Additive Models for Location Scale and Shape (GAMLSS) in R. *J. Stat. Softw.* **2008**, *23*, 1–46. [CrossRef]
40. Federal Highway Administration. *Manual on Uniform Traffic Control Devices for Streets and Highways (MUTCD)*, 11th ed.; Federal Highway Administration: Washington, DC, USA, 2023.

41. Dunn, P.K.; Smyth, G.K. Randomized Quantile Residuals. *J. Comput. Graph. Stat.* **1996**, *5*, 236–244. [CrossRef]
42. Salles, L.S.; Pereira, D.D.S.; Texeira, D.L.K.; Specht, L.P. Road Markings Retroreflectivity Experimental Assessment Observarions on Rainfall, Dirt, Retreflectometer Geometry and Minumum Requirements. In Proceedings of the 95th Annual Meeting of Transportation Research Board, Washington, DC, USA, 10–14 January 2016.